

TESTING COWLING'S ANTIDYNAMO THEOREM NEAR A ROTATING BLACK HOLE

AXEL BRANDENBURG¹

Received 1996 January 17; accepted 1996 May 1

ABSTRACT

The kinematic evolution of axisymmetric magnetic and electric fields is investigated numerically in Kerr geometry for a simplified Keplerian disk near a rotating black hole. In the cases investigated it is found that a magnetic field cannot be sustained against ohmic diffusion. In flat space this result is known as Cowling's antidynamo theorem. No support is found for the possibility that the gravitomagnetic dynamo effect of Khanna & Camenzind could lead to self-excited axisymmetric solutions. In practice, therefore, Cowling's antidynamo theorem may still hold in Kerr geometry, although here the original proof can no longer be applied.

Subject headings: accretion, accretion disks — black hole physics — magnetic fields — MHD — relativity

1. INTRODUCTION

Axisymmetric magnetic fields can generally be decomposed into a poloidal field and an azimuthal component. Differential rotation can stretch the poloidal field and convert it into an azimuthal field. This gives an efficient amplification of the magnetic field, but it requires the poloidal field as a source. However, in strictly two-dimensional geometry, there is no corresponding source for the poloidal field, which must eventually decay. The flow can only advect the poloidal field around, but, because of axisymmetry, it cannot stretch or amplify the poloidal field. This is known as Cowling's (1934) antidynamo theorem (see also Parker 1979).

In Kerr geometry, near a rotating black hole, the situation is different. The hole's rotation drags all physical objects near it into orbital motion in the same direction as the hole rotates. Physical quantities, such as electric and magnetic fields, are measured by fiducial observers (FIDOs), who are orbiting with angular velocity ω relative to a rigid coordinate grid. This frame-dragging effect acts in a similar way as ordinary differential rotation in nonrelativistic hydromagnetics and leads to field-line stretching. However, the frame dragging effect stretches not only magnetic fields but also electric fields. Khanna & Camenzind (1994, 1996, hereafter KC94 and KC96, respectively) pointed out that this could be important for Cowling's antidynamo theorem, because it leads to a back-reaction on the poloidal magnetic field: the poloidal electric field that is induced by the azimuthal magnetic field is stretched and converted into an azimuthal electric field, which could then induce a new poloidal magnetic field. Now, this new poloidal magnetic field could either enhance or diminish the original poloidal magnetic field. A simple sketch suggests that the original poloidal magnetic field is in fact enhanced by this sequence of events; see Figure 1.

In the chain of processes depicted above, only changes in the azimuthal electric and magnetic fields by stretching are considered, but the fields also change directly by induction. In particular, the poloidal magnetic field would induce a positive azimuthal electric field that tends to *oppose* the azimuthal electric field generated by the relativistic three-step process of stretch-induce-stretch. Thus, it is not clear whether the relativistic stretching effects would be able to dominate over the

ordinary induction effects to produce a self-excited dynamo (especially in the presence of additional field-line stretching by differential rotation in a surrounding accretion disk).

Based on numerical simulations, KC94 and KC96 suggested that a self-excited gravitomagnetic dynamo is indeed possible. However, they presented only two different cases, and it therefore remains unclear for which parameters (e.g., electrical conductivity, angular momentum of the black hole, geometry of the accretion flow) this process would work. In addition, certain features of their model might give rise to concern: neglect of the Faraday displacement current, numerical ripples near the horizon, and an initial magnetic field that is (almost) frozen into a highly conducting corona.

The purpose of this Letter is to investigate the possibility of dynamo action using an independent numerical method. A highly nonuniform mesh is adopted to resolve the accumulation of fields near the horizon, the Faraday displacement current is retained in some cases, and different conductivity profiles are examined.

2. MODEL AND NUMERICAL METHOD

There are many papers on what is now called black hole electrodynamics (e.g., Znajek 1977; Macdonald & Thorne 1982; Macdonald & Suen 1985; Park & Vishniac 1989), a topic that has recently also reached the textbook level (see Thorne, Price, & Macdonald 1986; Novikov & Frolov 1989). The standard procedure is to rewrite the covariant Maxwell equations in the form of evolution equations with respect to a universal time t . These equations have the familiar form

$$\frac{\partial \mathbf{B}}{\partial t} = \boldsymbol{\omega} e_{\hat{\phi}} (\mathbf{B} \cdot \nabla) \omega - c \nabla \times (\alpha \mathbf{E}), \quad (1)$$

$$\frac{\partial \mathbf{E}}{\partial t} = \boldsymbol{\omega} e_{\hat{\phi}} (\mathbf{E} \cdot \nabla) \omega + c \nabla \times (\alpha \mathbf{B}) - 4\pi \alpha \mathbf{j}, \quad (2)$$

together with $\nabla \cdot \mathbf{B} = 0$ and $\nabla \cdot \mathbf{E} = 4\pi \rho_e$, where ρ_e is the charge density. Axisymmetry has been assumed and Boyer-Lindquist coordinates are employed; r is the radial coordinate, θ is colatitude, ϕ is longitude, $e_{\hat{\phi}}$ is the unit vector in the ϕ -direction, and the hats indicate the physically measurable components of a vector. The differential operators are written in curvilinear coordinates with metric coefficients, $g_{rr}^{1/2}$, $g_{\theta\theta}^{1/2}$, and $g_{\phi\phi}^{1/2}$, that are functions of r and θ , which can be found in the publications mentioned above. \mathbf{E} and \mathbf{B} are the electric and

¹ NORDITA, Blegdamsvej 17, DK-2100 Copenhagen Ø, Denmark; now at the Department of Mathematics and Statistics, University of Newcastle upon Tyne, NE1 7RU, UK.

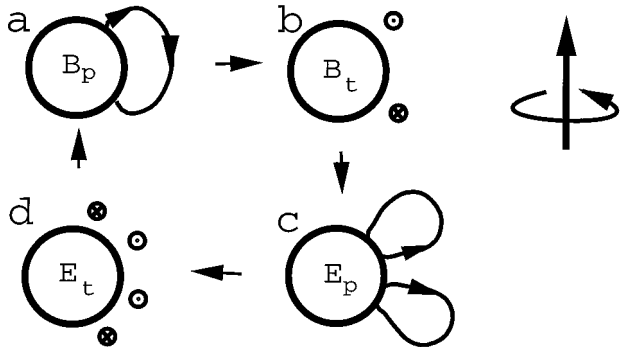


FIG. 1.—(a) Poloidal magnetic field pointing outward in the northern hemisphere becomes stretched into a negative azimuthal magnetic field. (b) This azimuthal magnetic field induces a poloidal electric field that goes from low to high latitudes. (c) This poloidal electric field becomes stretched into a negative azimuthal electric field at low latitudes and a positive electric field at high latitudes. (d) This toroidal electric field induces a new poloidal magnetic field that points outward at midlatitudes. If strong enough, this would enhance the original poloidal magnetic field.

magnetic fields, respectively, $\alpha = (-g'')^{-1/2}$ is the gravitational redshift factor, $\omega = g^{\phi\phi}/g''$ is the angular velocity caused by the frame dragging effect, $\varpi = g_{\phi\phi}^{1/2}$ is the circumference of a circle around the axis (divided by 2π), and c is the speed of light. (From now on, $c = G = 1$ is assumed, so length is measured in units of $[r] = GM/c^2$, time in units of $[t] = [r]/c$, and $[E] = [j][t] = [B] = B_0$, where B_0 is the initial magnetic field strength.) The current density j is governed by Ohm's law,

$$j = \sigma\gamma(E + v \times B) + \rho'_e \gamma v, \quad \text{with } \rho'_e \gamma = \rho_e - \sigma\gamma v \cdot E, \quad (3)$$

where σ is the conductivity, v is the bulk velocity of the plasma, $\gamma = (1 - v^2)^{-1/2}$ is the relativistic Lorentz factor, and ρ' and ρ are the charge densities in the rest frames of the plasma and the FIDO, respectively. In those cases where the Faraday displacement current $\partial E/\partial t$ is neglected, $\rho'_e = 0$ is assumed for consistency. (In the cases studied below ρ'_e turns out to be negligibly small; see Fig. 4.) The fields E and B are split into poloidal and toroidal fields, $E = E_p + E_t$ and $B = B_p + B_t$, where $E_t = E^\phi e_\phi$, $B_t = B^\phi e_\phi$, and $B_p = \nabla \times (A^\phi e_\phi)$, where A^ϕ is evolved in time to ensure that B is solenoidal.

Following the model assumptions made by KC96, the velocities v^ϕ and v_p are calculated in such a way that the angular momentum is 99% of its Keplerian value outside the marginally stable orbit r_{ms} , and equal to the value at r_{ms} for $r < r_{ms}$, where free fall with constant specific energy and angular momentum is assumed. The relevant formulae can be found in KC96 and Shapiro & Teukolsky (1983). The angular velocity is constant on spherical shells, and v_p is horizontal and confined to the disk using a Gaussian profile with a scale height of $H = 0.5M$, simulating an accretion flow in a disk. For the conductivity the prescription of KC96 is adopted: $(4\pi\sigma)^{-1} = 0.2H^2 v^\phi R^{-1} \exp(-z^2/H^2)$, where $z = r \cos \theta$ and $R = r \sin \theta$. For comparison, models with uniform conductivity and no accretion flow are also computed.

Equations (1)–(3) are solved using a third-order time step and (mixed centered/staggered) second-order differences. A tortoise coordinate,

$$x = r + r_H \ln(r/r_H - 1), \quad (4)$$

has been used, where $r_H = M + (M^2 - a^2)^{1/2}$ is the outer horizon, M is the mass of the black hole, and a is its angular momentum per unit mass in terms of $c^3/G = 1$. All r -

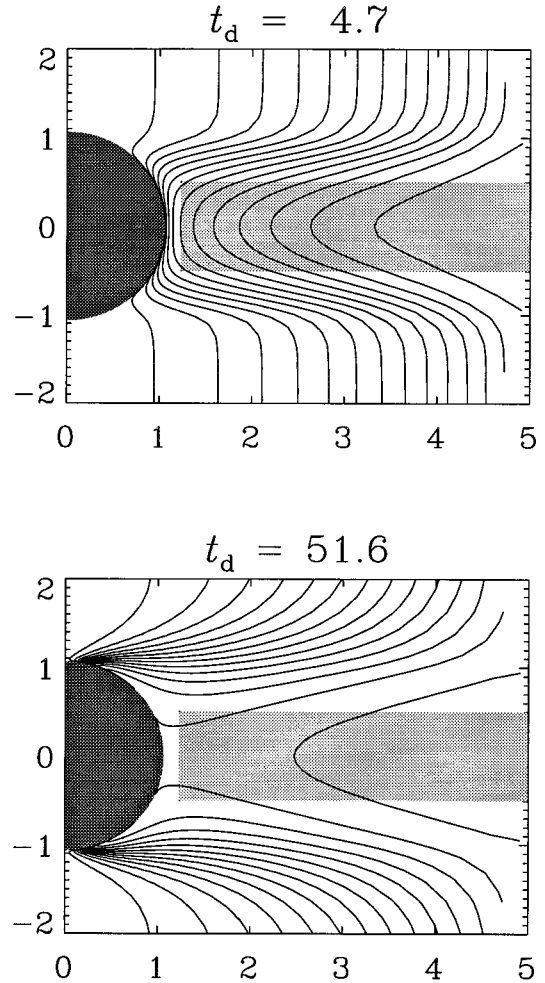


FIG. 2.—Poloidal field (contours of ϖA^ϕ) for three different times [in diffusion times $t_d = t/(4\pi\sigma_0)$, where $4\pi\sigma_0 = 42.6$ min ($4\pi\sigma$)]. Shaded areas indicate the extent of the hole ($r_H = 1.06$) and the disk ($r_{ms} = 1.237$, $H = 0.5$). $(4\pi\sigma_0)_{\max} = 5000$; 51×101 mesh points; $\partial E/\partial t = 0$.

derivatives are evaluated on a uniform grid in x and then multiplied by $dx/dr = (1 - r_H/r)^{-1}$.

The boundary conditions for B and E are formulated at the “stretched” horizon (Macdonald & Suen 1985), i.e., a very small distance above the actual horizon where α is still finite (in the present case, x_{\min} is varied between -20 and -12 , and so $\alpha_{\min} = 10^{-5}$ to 4×10^{-4}). On the boundary electromagnetic waves travel into the horizon, so the Poynting vector points into the hole with $B^\theta = E^\phi$ and $B^\phi = -E^\theta$, which, together with equation (2), leads to an outgoing wave condition for the horizontal components of E . No explicit condition for E^r is needed. On the outer boundary $B^\theta = B^\phi = 0$ is assumed (except in Cases A and B where a perfect conductor with $B^r = E^\theta = E^\phi = 0$ is assumed). In case C (below) the field parity was fixed by suitable boundary conditions at the equator, so that B has even or odd symmetry. The code was tested for $\sigma = 0$ by reproducing the relaxation of an initially radial magnetic field to a steady vertical field solution that is known analytically (Wald 1974). For finite conductivity and with Keplerian differential rotation the code was tested by computing $\alpha\Omega$ dynamo action in Schwarzschild geometry, giving results in qualitative agreement with expectations. The effective DC resistivity of the black hole of ≈ 377 ohms was verified

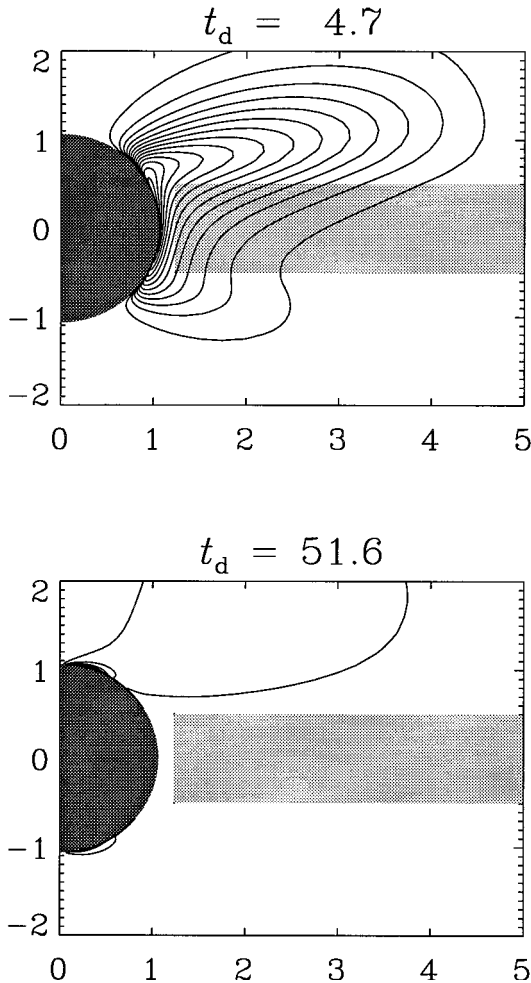


FIG. 3.—Poloidal field at different times in the case without imposed magnetic field. Dotted contours indicate opposite orientation. The field dies out and is absorbed by the black hole. $(4\pi\sigma_0)_{\max} = 500$; 51×101 mesh points; $\partial\mathbf{E}/\partial t = 0$.

numerically by applying an electric field and measuring the resulting current (see Fig. 15 of Thorne et al. 1986).² For a parameter survey, a resolution of 41×21 mesh points in the r - and θ -directions proved to be sufficient; comparison with 81×51 mesh points gave very similar results. For those calculations where $\partial\mathbf{E}/\partial t = 0$ is assumed, the \mathbf{E} -field is obtained from equation (3).

3. RESULTS

The results presented here are for $M = 1$, $a = 0.998$ (corresponding to maximal rotation; cf. Thorne 1974), and $r_{\max} = 5$.

Case A.—In order to compare with the model of KC94, $\partial\mathbf{E}/\partial t$ is neglected and an initially vertical magnetic field with a weak toroidal field is adopted such that the initial field parity is mixed. Following KC94 (and R. Khanna 1996, private communication), the conductivity away from the disk plane was limited to $4\pi\sigma = 5000$. There is a strong increase of the

² Note that KC96 erroneously adopted an enhanced magnetic diffusion on the stretched horizon to mimic the ≈ 377 ohms. R. Khanna (1996, private communication) pointed out that this was the reason for the ripples found in KC94 and KC96.

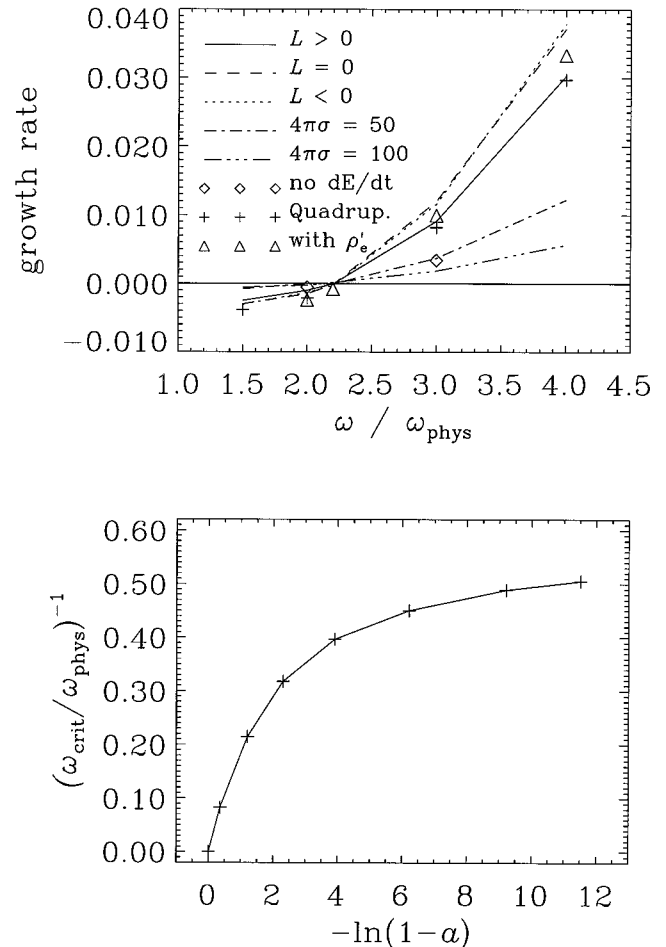


FIG. 4.—*Top:* Growth rate vs. $\omega/\omega_{\text{phys}}$. The angular momentum density L of the disk is +99%, 0, and -99% of its Keplerian value, and $4\pi\sigma = 20$. Comparison is made with $4\pi\sigma = 50$ and 100 ($L > 0$), where $\partial\mathbf{E}/\partial t$ is either included or neglected (for $4\pi\sigma = 50$). The difference between dipole-like and quadrupole-like solutions is negligible, and so is the inclusion of the ρ'_e term. *Bottom:* Inverse threshold $(\omega_{\text{crit}}/\omega_{\text{phys}})^{-1}$ for different values of a . 41×21 meshpoints.

magnetic field due to the shear between the disk and the corona; see Figure 2. Note that at all times the field remains smooth. As time goes on, the field in the disk plane is advected into the hole and does not accumulate near the horizon; this is unlike the behavior in KC94.

Case B.—In the previous case the field was (almost) frozen into a highly conducting corona and acted like an *imposed* field. This is unsuitable for the study of dynamo action. Therefore, the conductivity outside the disk is now limited to $4\pi\sigma = 500$, and the initial field is confined to the disk. In order to allow for mixed parity, the initial field is zero in the lower disk plane. The field increased initially due to shear, but at later times it decayed due to dissipation or because it was simply absorbed by the black hole; see Figure 3. Thus, there is no self-excited dynamo.

Case C.—In order to understand why the gravitomagnetic dynamo effect of KC94 does not operate in the present case, the angular velocity ω of the frame dragging was increased *artificially* above its physical value ω_{phys} . This computational device helps to locate the dynamo effect in parameter space. In the absence of a radial accretion flow and for uniform con-

ductivity, there is a self-excited solution for $\omega_{\text{crit}}/\omega_{\text{phys}} \approx 2.2$; see Figure 4, *top panel*. Radial accretion impedes dynamo action ($\omega_{\text{crit}}/\omega_{\text{phys}} \approx 3.1$), but the value and profile of σ have very little effect on the threshold. Even for a very high angular momentum of the black hole ($a = 0.999999$), $\omega_{\text{crit}}/\omega_{\text{phys}}$ is well above unity (≈ 1.9); see Figure 4, *bottom panel*. This suggests that the threshold for dynamo action cannot be attained for any physically reasonable input parameters.

In Kerr geometry, Cowling's proof cannot be applied: the toroidal current induced at the neutral O-type line could *in principle* be supported by the $E_p \cdot \nabla\omega$ term. In order that $|E^\phi|$ does not vanish, one has to require that $\partial(E^\phi)^2/\partial t \geq 0$, and, from equation (2), $E^\phi E_p \cdot \nabla\omega > 0$. Inspection of solutions with $\omega = \omega_{\text{phys}}$ showed, however, that this is not the case in the examples considered here. This is because the negative toroidal electric field in Figure 1d is dominated by the positive electric field induced by B_p . Therefore, $E^\phi E_p > 0$ in the equatorial plane, and, because $\nabla_r \omega < 0$, $E^\phi E_p \cdot \nabla\omega < 0$. (On

the other hand, for $\omega \geq \omega_{\text{crit}}$ the sign of $E^\phi E_p \cdot \nabla\omega$ is indeed positive, as expected.)

4. CONCLUSIONS

The present calculations suggest that the gravitomagnetic dynamo effect of KC94 and KC96 does *not* lead to self-excited solutions in Keplerian disks surrounding rotating black holes. The neglect of the Faraday displacement current and the charge density proves to be a good approximation in the cases considered here. Although axisymmetric dynamo action seems not to occur, it is quite clear, however, that accretion disks will always be magnetized by *three-dimensional* dynamo action (cf. Brandenburg et al. 1995).

A. B. thanks Ramon Khanna, David Moss, Åke Nordlund, and Ulf Torkelsson for illuminating discussions and comments on the manuscript.

REFERENCES

- Brandenburg, A., Nordlund, Å., Stein, R. F., & Torkelsson, U. 1995, ApJ, 446, 741
 Cowling, T. G. 1934, MNRAS, 94, 39
 Khanna, R., & Camenzind, M. 1994, ApJ, 435, L129 (KC94)
 ———. 1996, A&A, 307, 665 (KC96)
 Macdonald, D. A., & Suen, W.-M. 1985, Phys. Rev. D, 32, 848
 Macdonald, D. A., & Thorne, K. S. 1982, MNRAS, 198, 345
 Novikov, I. D., & Frolov, V. P. 1989, Physics of Black Holes (Dordrecht: Kluwer)
 Park, S. J., & Vishniac, E. T. 1989, ApJ, 337, 78
 Parker, E. N. 1979, Cosmical Magnetic Fields (Oxford: Clarendon)
 Shapiro, S. A., & Teukolsky, S. L. 1983, Black Holes, White Dwarfs, and Neutron Stars (New York: Wiley)
 Thorne, K. S. 1974, ApJ, 191, 507
 Thorne, K. S., Price, R. H., & Macdonald, D. A. 1986, Black Holes: The Membrane Paradigm (New Haven: Yale Univ. Press)
 Wald, R. M. 1974, Phys. Rev. D, 10, 1680
 Znajek, R. L. 1977, MNRAS, 179, 457